International Journal of Innovative
Computing, Information and Control
Volume **15**, Number **3**, June **2019**

 ISSN 1349-4198
pp. **969–982**

A CROSS-CONNECTED CHARGE PUMP FOR ENERGY HARVESTING APPLICATIONS

Wanlok Do[1], Haruka Fujisaki[1], Farzin Asadi[2] and Kei Eguchi[1]

[1]Department of Information Electronics
Fukuoka Institute of Technology
3-30-1 Wajirohigashi, Higashi-ku, Fukuoka 811-0295, Japan
dwlkiss88@gmail.com; s14f2045@bene.fit.ac.jp; eguti@fit.ac.jp

[2]Mechatronics Engineering Department
Kocaeli University
Umuttepe Yerleşkesi 41380, Kocaeli, Turkey
farzin.asadi@kocaeli.edu.tr

Received September 2018; revised January 2019

Abstract. *Energy harvesting is a process of capturing, storing and converting external energy from ambient energy. The energy harvesting systems commonly use a switched-mode power supply (SMPS) to convert energy harvested from the ambient energy. Therefore, the power converter is an essential component in terms of developing efficient energy harvesting systems. Among SMPS, inductor-less converter can be a solution. This paper suggests a new topology of charge pumps by cross-connecting two of them for efficient energy harvesting systems. With the cross-connected structure, the new topology transfers a stepped-up output to the output capacitor and load in all operation periods. This operation way can improve the power efficiency of the proposed charge pump and also decrease the internal resistance and the output capacitor's capacitance of it. The performance of the proposed charge pump is verified by comparing with two conventional charge pumps, which is based on simulation program with the integrated circuit emphasis (SPICE) simulations and theoretical analysis. Moreover, we demonstrated the feasibility of the proposed one through the experimental circuit built on a breadboard. The proposed charge pump helps develop efficient energy harvesting systems.*
Keywords: Charge pump, Cross-connected topology, Energy harvesting, Inductor-less converters, Power converters

1. **Introduction.** Energy harvesting is a process of capturing, storing and converting external energy, sources of which are solar energy, wind energy, kinetic energy, etc. Utilizing the external energy from them, the energy harvesting systems are considered as one of the eco-friend technologies. The representative applications using the energy harvesting systems are wearable devices and wireless sensor networks. To harvest ambient energy, the energy harvesting systems employ photovoltaics (PVs) technology, piezoelectric effect, Peltier effect and so on. The energy collecting devices in the energy harvesting systems are commonly designed by using a switched-mode power supply (SMPS) to convert energy harvested from the ambient energy. Therefore, the power converter is an essential component in terms of developing efficient energy harvesting systems.

Among the types of SMPS, the inductor-less power converters, the so called switched-capacitor (SC) power converters or charge pumps, can be a suitable solution, because the absence of magnetic components provides strong merits such as the reduction of the circuit size and the minimization of electromagnetic interference (EMI) noises. As well as

DOI: 10.24507/ijicic.15.03.969

these strengths, SC power converters can work in four types of power conversions: DC to DC [1,2,30], DC to AC [3,28], AC to DC [4,27] and AC to AC [5,29]. In this paper, we focus on the power conversion type of DC to DC.

Dickson charge pump was suggested in 1976 [6]. Since then, many different types of the SC power converters have been proposed such as Ioinovici SC [7], Fibonacci sequence [8-11], switched capacitor voltage multiplier (SCVM) [12], and ring [13,14]. However, those common topologies are not designed only for energy harvesting systems. In order to make SC power converters fit in energy harvesting systems, many attempts have been undertaken in the design and rearrangement of efficient SC power converters. For example, Doms et al. [15,16] and Yun et al. [17,18] suggested a charge pump for thermoelectric generators (TEGs). The proposed charge pump in [15-18] generates a stepped-up output in only half of the operation period, which requires an output capacitor of high capacitance to reduce its output ripple. To supply the stable input power to energy harvesting systems, Eguchi et al. [19,20] combined a clean energy source (input source) and a battery source. While supplying the stable input to them, the multiple-input charge pump in [19,20] makes their size bigger. In a bid to reduce the output ripple and to improve power efficiency, a split-merge charge pump was proposed by Wang et al. [21,22]. The suggested charge pump in [21,22] requires multi-phase clock pulse for its operation, which leads to the complex control way. Furthermore, due to the characteristic of parallel-connected topology [23-25], the circuit size, such as the suggested charge pump [21,22], becomes large.

In this paper, a novel charge pump is proposed in order to realize efficient energy harvesting systems. It is 'cross-connected topology' that is a structural feature of the proposed charge pump. This structural feature allows the proposed charge pump to have the following advantages: 1) a stepped-up mode in all operation periods; 2) high conversion gain; 3) small internal resistance. With those strengths, the proposed charge pump can achieve higher power efficiency and decrease the capacitance of the output capacitor than conventional inductor-less power converters. The proposed charge pump and the conventional inductor-less converters are compared through simulation program with integrated circuit emphasis (SPICE) simulations and theoretical analysis so as to verify the performance of the proposed charge pump.

Originally, the idea of 'cross-connected topology' is based on our previous study [26]. The previous study [26] suggested the basic idea of cross connecting two charge pumps and then compared the proposed and conventional charge pump. This paper shows the workability of the proposed charge pump through the experiment in Section 4. Moreover, the comparison is implemented with two conventional charge pumps in order to verify the performance of the proposed charge pump more objectively.

This paper is organized as follows. In Section 2, we present the difference of circuit structure and operation between the proposed charge pump and conventional charge pumps. In Section 3, we clarify the characteristics of the proposed charge pump by theoretical analysis. In Section 4, we simulate the proposed charge pump and the conventional charge pumps, through which we demonstrate the effectiveness of the proposed charge pump. Then, we confirm the feasibility of the proposed charge pump by experimental results. In Section 5, we summarize this study.

2. Circuit Configuration.

2.1. Conventional charge pump.

Figure 1 shows the circuit configuration of the conventional charge pump [15-18]. The conventional charge pump is operated by controlling electric switches S_1 and S_2 with non-overlapped clock pulses (Φ_1 and Φ_2). The relationship

between the input and the output voltage is shown as (1).

$$V_{out} = (N + 1)V_{in}. \tag{1}$$

In (1), N is the parameter that represents the number of stages consisting of 1 capacitor and 3 switches. The parameter N in the case of Figure 1 is 3. According to (1), the conventional charge pump has the proportional relationship between its step-up gain and the number of stages.

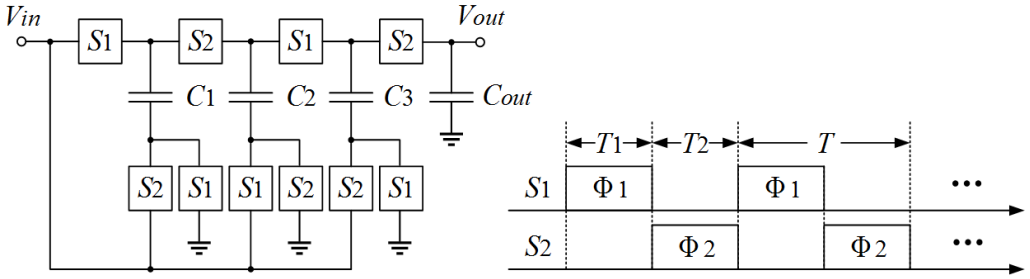

FIGURE 1. Circuit and operation clock pulses (Φ_1 and Φ_2) of the conventional charge pump

The conventional charge pump provides the stepped-up voltage to the output load from the output capacitor C_{out} during T_1. On the other hand, the conventional charge pump charges and discharges the output capacitor during the operation period T_1 and T_2 respectively. This operation way requires an output capacitor of high capacitance to reduce output ripple. Even though a multistep split-merge charge transfer operation [21,22] can be a solution to improve the output ripple and power efficiency of the conventional charge pump, the complex circuit control is demanded in the sense that the suggested topology in [21,22] is operated in multi-phase clock pulses. Furthermore, the circuit size of the suggested charge pump [21,22] becomes large due to the characteristic of parallel-connected topologies [23-25].

2.2. **Proposed cross-connected charge pump.** Figure 2 describes the circuit configuration of the proposed cross-connected charge pump. The proposed charge pump consists

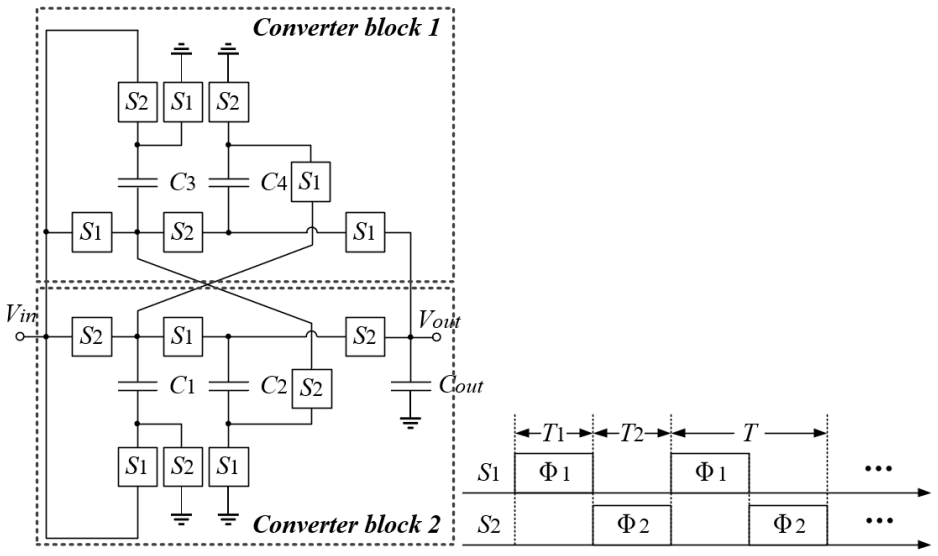

FIGURE 2. Circuit and operation clock pulses (Φ_1 and Φ_2) of the proposed charge pump with 4 times step-up gain

of two converter blocks that is cross-connected. The proposed charge pump is operated by controlling electric switches S_1 and S_2 with non-overlapped two clock pulses (Φ_1 and Φ_2). Through the structural feature of the cross-connection, the sub-circuit in each operation period (T_1 and T_2) has the symmetrical structure. The relationship between the input and the output voltage is shown as (2).

$$V_{out} = 2NV_{in}. \tag{2}$$

The distinguishing feature of the proposed charge pump is the operation way of offering the stepped-up voltage to the output load. The proposed charge pump transfers the stepped-up voltage to the output load during all operation periods, differently from the conventional charge pump. These features allow the proposed charge pump to reduce the output capacitor's capacitance, the output ripple and the number of stages. These reduced factors lead to higher power efficiency and smaller circuit size than the conventional one.

3. **Theoretical Analysis.**

3.1. **Proposed charge pump.** To elucidate the circuit characteristics, we theoretically analyze the proposed charge pump based on the four-terminal equivalent model in steady state [19,20] in Figure 3. The explanation of the parameters in Figure 3 is as follows. m is the step-up ratio (conversion ratio) of an ideal transformer. I_{in}, V_{in}, I_{out} and V_{out} are the input current and voltage, and the output current and voltage, respectively. R_L and R_{SC} are the output load and the internal resistor that is named the SC resistance. In the four-terminal equivalent model in steady state, the main task is to derive the R_{SC} that is the component to consume energy with R_L. By using R_{SC}, we can theoretically examine the proposed charge pump to derive the power efficiency and the output voltage.

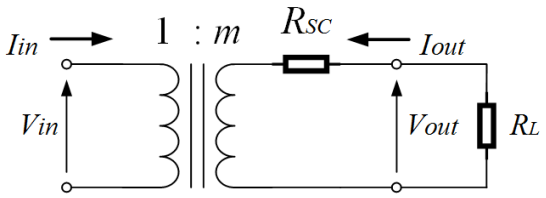

FIGURE 3. Four-terminal equivalent model of charge pump in steady state

Figure 4 shows equivalent circuits of the proposed charge pump in steady state. As mentioned in Section 2, the equivalent circuits have the feature of the symmetrical structure. In Figure 4, the parameter $\Delta q_{T_i,V_{in}\ or\ V_{out}}$ represents the amount of the electric charges of the input or output in state-T_i ($i = 1, 2$). The parameter R_{on} represents the equivalent resistance of closed switches. The four-terminal equivalent model in steady state satisfies the ampere-second balance principle, which means that the amount of charged and discharged electric charges is the same. Therefore, we can obtain the following equation.

$$\Delta q^k_{T_1} + \Delta q^k_{T_2} = 0, \tag{3}$$

where the parameter $\Delta q^k_{T_i}$ represents the amount of the k-th ($k = 1, 2, 3, 4, out$) capacitor (C_k)'s electric charges in state-T_i ($i = 1, 2$).

In the theoretical analysis, the duty ratio of the operation period is set to 50%. The operation period, state-T_i ($i = 1, 2$), is satisfied with (4).

$$T = T_1 + T_2 \quad \text{and} \quad T_1 = T_2 = \frac{T}{2}. \tag{4}$$

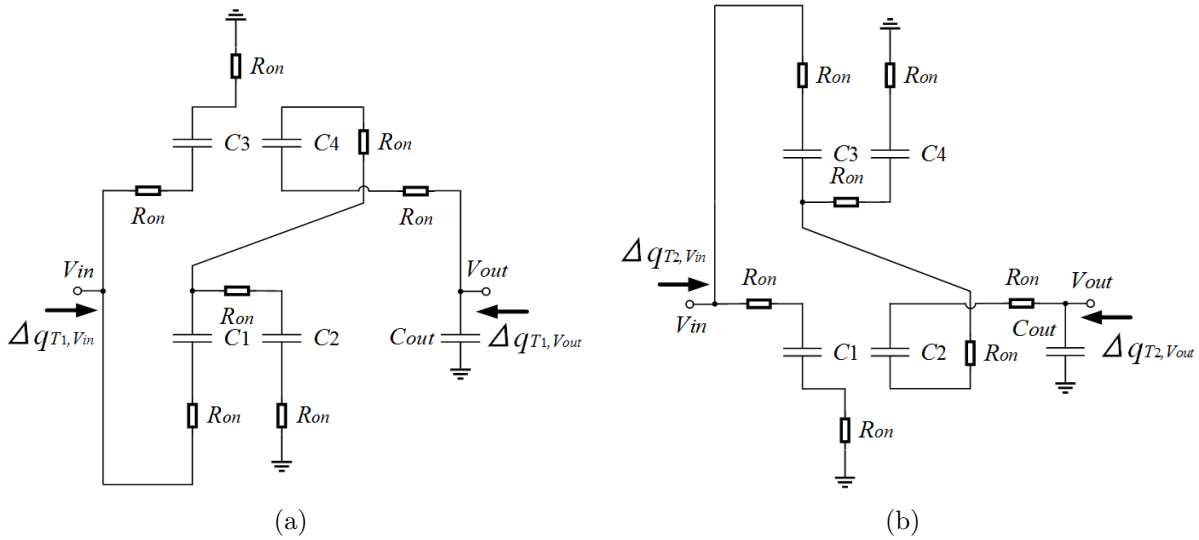

FIGURE 4. Equivalent circuits of the proposed charge pump in steady state: (a) state-T_1 and (b) state-T_2

The amount of electric charges in State-T_1, $\Delta q_{T_1,V_{in}}$ and $\Delta q_{T_1,V_{out}}$ are obtained as shown in (5), which is based on Kirchhoff's current law.

$$\begin{aligned} \Delta q_{T_1,V_{in}} &= \Delta q^3_{T_1} - \Delta q^1_{T_1}, \\ \Delta q_{T_1,V_{out}} &= \Delta q^4_{T_1} + \Delta q^{out}_{T_1}, \\ \text{and} \quad \Delta q^4_{T_1} &= \Delta q^1_{T_1} + \Delta q^2_{T_1}. \end{aligned} \tag{5}$$

Likewise, by using Kirchhoff's current law, the amount of electric charges in State-T_2, $\Delta q_{T_2,V_{in}}$ and $\Delta q_{T_2,V_{out}}$, are obtained as shown in (6).

$$\begin{aligned} \Delta q_{T_2,V_{in}} &= \Delta q^1_{T_2} - \Delta q^3_{T_2}, \\ \Delta q_{T_2,V_{out}} &= \Delta q^2_{T_2} + \Delta q^{out}_{T_2}, \\ \text{and} \quad \Delta q^2_{T_2} &= \Delta q^3_{T_2} + \Delta q^4_{T_2}. \end{aligned} \tag{6}$$

In a theoretical analysis, we assume that the voltage and current of the input and output maintain the stable state, which means that there is no change in the input and output. Therefore, the relationship between the input and output average current can be expressed as shown in (7).

$$\begin{aligned} I_{in} &= \frac{\Delta q_{V_{in}}}{T} = \frac{\Delta q_{T_1,V_{in}} + \Delta q_{T_2,V_{in}}}{T} \\ \text{and} \quad I_{out} &= \frac{\Delta q_{V_{out}}}{T} = \frac{\Delta q_{T_1,V_{out}} + \Delta q_{T_2,V_{out}}}{T}. \end{aligned} \tag{7}$$

In (7), $\Delta q_{V_{in}}$ and $\Delta q_{V_{out}}$ are the electric charges amount of the input and output, respectively. The relationship between the input and output average currents including conversion ratio can be derived as shown in (8) by substituting (3)-(6) into (7).

$$I_{in} = -4I_{out}. \tag{8}$$

According to (8), the parameter m in Figure 3 is 4.

The next step is to analyze the energy consumption except for the output load in one operation period and to derive the R_{SC}. The energy consumption in State-T_1 is obtained

as (9).

$$W_{T_1} = \frac{\left(\Delta q^1_{T_1}\right)^2}{T_1} R_{on} + \frac{\left(\Delta q^2_{T_1}\right)^2}{T_1} 2R_{on} + \frac{\left(\Delta q^3_{T_1}\right)^2}{T_1} 2R_{on} + \frac{\left(\Delta q^4_{T_1}\right)^2}{T_1} 2R_{on}. \tag{9}$$

The total energy consumption in one operation period can be derived as (10) since the proposed charge pump has the symmetrical structure as shown in Figure 4.

$$W_T = \frac{\left(\Delta q_{V_{out}}\right)^2}{T} 16R_{on}. \tag{10}$$

In the interim, (11) can be defined for the relationship of the energy consumption from the four-terminal equivalent model in Figure 3, differently from (10).

$$W_T = \frac{\left(\Delta q_{V_{out}}\right)^2}{T} R_{SC}. \tag{11}$$

Therefore, we can confirm by comparing (10) and (11) that the parameter R_{SC} is $16R_{on}$. Through above steps, we can derive the K-matrix of the proposed charge pump as (12), which includes the information of the relation of I/O, the conversion ratio and the internal resistance.

$$\begin{bmatrix} V_{in} \\ I_{in} \end{bmatrix} = \begin{bmatrix} 1/4 & 0 \\ 0 & 4 \end{bmatrix} \begin{bmatrix} 1 & 16R_{on} \\ 0 & 1 \end{bmatrix} \begin{bmatrix} V_{out} \\ -I_{out} \end{bmatrix}. \tag{12}$$

The parameter $\eta_{\max}$ and $V_{\max}$, maximum efficiency and output voltage, are obtained as (13) by applying the voltage division principle in Figure 3

$$\eta_{\max} = \frac{R_L}{16R_{on} + R_L} \quad \text{and} \quad V_{\max} = \left(\frac{R_L}{16R_{on} + R_L}\right) \times 4V_{in}. \tag{13}$$

3.2. **Comparison.** The comparison of $\eta_{\max}$ and $V_{\max}$ with other conventional charge pumps is shown in Table 1. In Table 1, the theoretical analysis of two conventional charge pumps is given in Appendix. As shown in Table 1, the proposed charge pump is able to have higher $\eta_{\max}$ and $V_{\max}$ than the conventional ones.

TABLE 1. Maximum power efficiency and output voltage of the charge pumps

	Power efficiency	Output voltage
Proposed charge pump	$\frac{R_L}{16R_{on} + R_L}$	$\left(\frac{R_L}{16R_{on} + R_L}\right) \times 4V_{in}$
Conventional charge pump [17,18]	$\frac{R_L}{20R_{on} + R_L}$	$\left(\frac{R_L}{20R_{on} + R_L}\right) \times 4V_{in}$
Series-parallel charge pump [21,22]	$\frac{R_L}{38R_{on} + R_L}$	$\left(\frac{R_L}{38R_{on} + R_L}\right) \times 4V_{in}$

Table 2 shows the comparison of the number of circuit components with other conventional charge pumps. As shown in Table 2, the number of circuit components of the proposed converter is bigger than that of two conventional ones, whereas having the weakness of the circuit size, the proposed charge pump has the strength of providing the stepped-up voltage to the output load during all operation periods and reducing the capacitance of the output capacitor. This strength can contribute to the proposed charge pump in having higher response speed and smaller occupational chip area.

TABLE 2. The number of circuit components of the charge pumps

	Number of switches	Number of capacitors
Proposed charge pump	14	5 ($C_1 = \cdots = C_4 = C_{out} = 200$ pF)
Conventional charge pump [17,18]	10	4 ($C_1 = \cdots = C_3 = 200$ pF and $C_{out} = 5$ nF)
Series-parallel charge pump [21,22]	11	4 ($C_1 = \cdots = C_3 = 200$ pF and $C_{out} = 5$ nF)

4. **Simulation and Experimental Results.**

4.1. **Simulation results.** We simulate the proposed and conventional charge pumps with SPICE simulator in order to verify the performance of the proposed one. This simulation is implemented with the conditions as follows [21,22]: the input voltage is 400 mV, the on-resistance of electric switches is 1 Ω, all capacitances of the proposed charge pump's capacitors are 200 pF, the capacitances of the conventional charge pumps' capacitor are $C_1 = C_2 = C_3 = 200$ pF and $C_{out} = 5$ nF, the operation clock frequency f is 1 MHz, and the duty ratio of the operation clock is 50%, which indicates that T_1 and T_2 are 5 μs.

Figure 5 describes the simulation result of the output voltages of the charge pumps at different output power. We confirm that the proposed charge pump has higher output voltage than the conventional ones. Particularly, the output voltage of the proposed charge pump is maximum 80 mV higher at the output power of 30 μW.

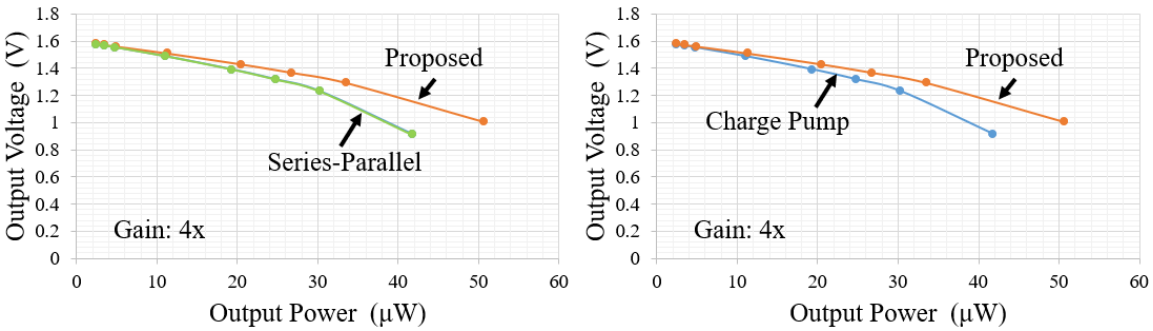

FIGURE 5. Simulation result of output voltage at different output power: the proposed charge pump vs. the series-parallel one on the left and the proposed charge pump vs. the conventional one on the right

Figure 6 depicts the simulation result of the power efficiency of the charge pumps at different output power. As shown Figure 6, the proposed charge pump has the highest power efficiency among others in the case of the output power over 10 W. Concretely, the power efficiency of the proposed charge pump is maximum 5% higher at the output power of 30 μW.

Figure 7 shows the simulation result for the response speed of the charge pumps with the output load of 10 kΩ. Through the simulation result in Figure 7, the proposed charge pump is confirmed to have the fastest response speed among others. The reason of that is because the proposed charge pump has the operation feature of the symmetrical structure and is able to reduce the capacitance of the output capacitor. The proposed charge pump has the improved settling time of about 150 μs at the above-mentioned simulation conditions.

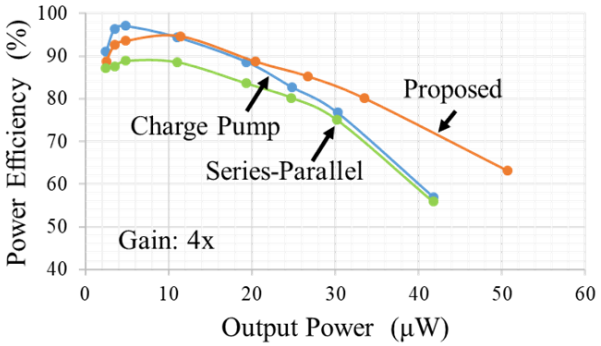

FIGURE 6. Simulation result of power efficiency at different output power

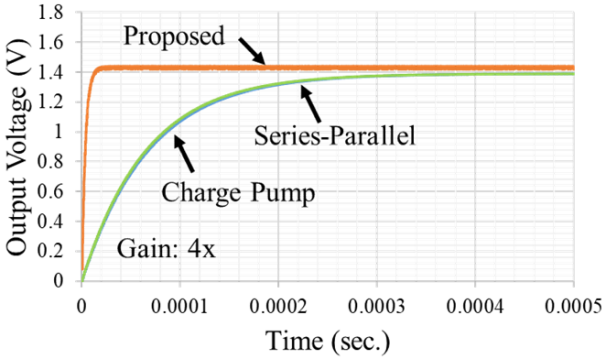

FIGURE 7. Simulation result of response speed

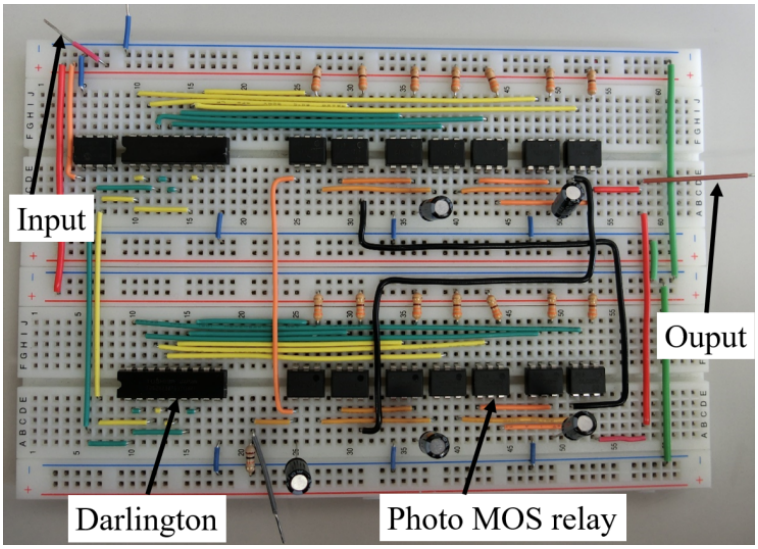

FIGURE 8. Experimental circuit on breadboard

4.2. **Experimental results.** We verify the feasibility of the proposed charge pump through the experimental circuit as shown in Figure 8. The experimental circuit of the proposed charge pump was constructed on a breadboard with circuit components enumerated in Table 3. In the experimental circuit, the photo MOS relays (electric switches) are controlled by the signals (clock pulses) from the Darlington transistor arrays connected to the PIC12F629-I/P or the microcontroller. The reason why Darlington transistor arrays are used in the experiments is to drive safely the photo MOS relays.

TABLE 3. The experimental circuit components

Parts	Components	Models/Values
Main block	Switch/On resistance	AQV212/0.83 Ω
	Capacitor	33 μF
Control block	Micro controller	PIC12F629-I/P
	Darlington driver IC	TD6203APG
	Current control resistance	330 Ω
Output load	Resistance	10 kΩ

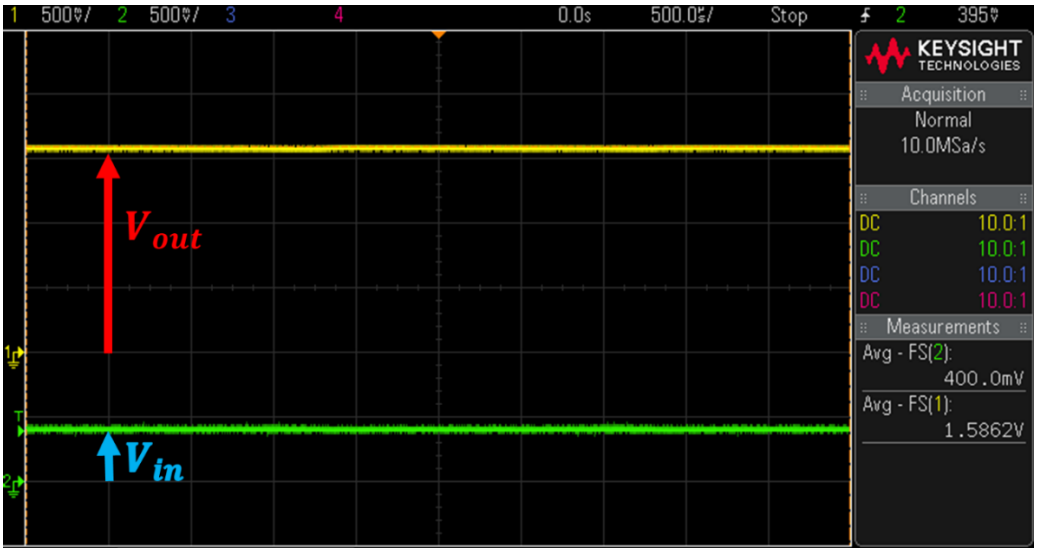

FIGURE 9. Experimental waveforms of output voltage

The experimental output voltage is given in Figure 9. The experimental setup is as follows: the output load of 10 kΩ, the input voltage of 400 mV and the clock pulses of the operation period (50% duty ratio) of 4 ms. As Figure 9 shows, the output voltage of the proposed one is about 1.5862 V. It is the negligible error of 0.0117 that is the difference between the theoretical result (1.5979 V) and the experimental output voltage.

5. **Conclusions.** This paper has proposed a new design of a charge pump named "cross-connected charge pump" for energy harvesting systems. The reason of this nomenclature is because the proposed charge pump has the cross-connected two converter blocks. The structural feature contributes the proposed charge pump to have smaller internal resistance and smaller capacitance of the output capacitor than other conventional charge pumps. To verify the performance of the proposed charge pump, we implemented the theoretical analysis and SPICE simulations. The result of them confirmed that the proposed charge pump has the following strengths: first, maximum 5% higher power efficiency and maximum 80 mV output voltage than other conventional charge pumps at the output power of 30 μW; second, the improved settling time of about 150 μs at the output load of 10 kΩ. The result of the experiment demonstrated the feasibility of the proposed charge pump with the negligible error of 0.0117. It is left for a future study to apply the proposed charge pump to energy harvesting systems and to implement it into an IC package.

REFERENCES

[1] W. Do and K. Eguchi, A control way of a Fibonacci sequence switched capacitor DC-DC converter for higher power efficiency, *ICIC Express Letters*, vol.12, no.1, pp.55-60, 2018.

[2] S. Pongswatd, K. Smerpituk, K. Eguchi and H. Sasaki, Design of step up and down bi-directional switched capacitor DC-DC converter, *ICIC Express Letters*, vol.6, no.2, pp.529-534, 2012.
[3] K. Eguchi, K. Abe, W. Do and H. Sasaki, Design of an inductor-less DC-AC inverter using a step-down Fibonacci sequence generator, *ICIC Express Letters*, vol.10, no.8, pp.1951-1956, 2016.
[4] K. Abe, I. Oota, W. Do, S. Kittipanyangam and K. Eguchi, Design of a step-down switched-capacitor AC/DC converter with series-connected converter blocks, *ICIC Express Letters*, vol.10, no.8, pp.2045-2050, 2016.
[5] K. Eguchi, F. Asadi, H. Abe, T. Ishibashi and H. Sasaki, Development of a simple direct switched-capacitor AC-AC converter using cascade connection, *International Journal of Innovative Computing, Information and Control*, vol.14, no.6, pp.2335-2342, 2018.
[6] J. K. Dickson, On-chip high voltage generation in nMOS integrated circuits using an improved voltage multiplier technique, *IEEE J. Solid-State Circuits*, vol.SSC-11, no.2, pp.374-378, 1976.
[7] O. C. Mak, Y. C. Wong and A. Ioinovici, Step-up DC power supply based on a switched-capacitor circuit, *IEEE Trans. Industrial Electronics*, vol.42, no.1, pp.90-97, 1995.
[8] F. Ueno, T. Inuoe, I. Oota and I. Harada, Emergency power supply for small computer systems, *Proc. of IEEE International Sympoisum on Circuits and Systems*, pp.1065-1068, 1991.
[9] M. S. Makowski and D. Maksimovic, Performance limits of switched-capacitor DC-DC converter, *Proc. of PESC'95 – Power Electronics Specialist Conference*, vol.2, pp.1215-1221, 1995.
[10] M. S. Makowski, Realizability conditions and bounds on synthesis of switched-capacitor DC-DC voltage multiplier circuits, *IEEE Trans. Circuits and Systems I: Fundamental Theory and Applications*, vol.44, no.8, pp.684-691, 1997.
[11] L. Liu and Z. Chen, Analysis and design of Makowski charge-pump cell, *Proc. of the 6th International Conference on ASIC*, vol.1, pp.497-502, 2005.
[12] Y. H. Chang, Variable-conversion-ratio switched-capacitor-voltage-multiplier/divider DC-DC converter, *IEEE Trans. Circuits and Systems I: Regular Papers*, vol.58, no.8, pp.1944-1957, 2011.
[13] N. Hara, I. Oota and F. Ueno, A new ring type switched-capacitor DC-DC converter with low inrush current and low ripple, *Proc. of the 29th Annual IEEE Power Electronics Specialists Conference*, pp.1536-1542, 1998.
[14] S. Terada, I. Oota, K. Eguchi and F. Ueno, A ring type switched-capacitor (SC) programmable converter with DC or AC input/DC or AC output, *Proc. of the 47th Midwest Symposium on Circuits and Systems*, pp.I-29-I-32, 2004.
[15] I. Doms, P. Merken, C. V. Hoof and R. P. Mertens, Capacitive power management circuit for micropower thermoelectric generators with a 1.4μA controller, *IEEE Journal of Solid-State Circuits*, vol.44, no.10, pp.2824-2833, 2009.
[16] I. Doms, P. Merken, C. V. Hoof and R. P. Mertens, Capacitive power-management circuit for micropower thermoelectric generators with a 2.1μW controller, *Proc. of IEEE International Solid-State Circuits Conference*, pp.300-301, 2008.
[17] G. S. Yun, K. S. Leong and M. F. B. A. Rahman, Development of charge pump circuit using multivibrator for thermoelectric generator, *Proc. of IEEE International Conference on Power and Energy*, pp.434-438, 2016.
[18] G. S. Yun, K. S. Leong and M. F. B. A. Rahman, Development of self-powered thermoelectric based RF transmitter circuit, *Proc.of IEEE International Conference on Power and Energy*, pp.439-443, 2016.
[19] K. Eguchi, T. Sugimura, S. Pongswatd, K. Tirasesth and H. Sasaki, Design of a multiple-input parallel SC DC-DC converter and its efficiency estimation method, *ICIC Express Letters*, vol.3, no.3(A), pp.531-536, 2009.
[20] K. Eguchi, K. Fujimoto and H. Sasaki, A hybrid input charge-pump using micropower thermoelectric generators, *IEEJ Trans. Electrical and Electronic Engineering*, vol.7, no.4, pp.415-422, 2012.
[21] Y. Wang, N. Yan, H. Min and C. J. R. Shi, A high-efficiency split-merge charge pump for solar energy harvesting, *IEEE Trans. Circuits and Systems II: Express Briefs*, vol.64, no.5, pp.545-549, 2017.
[22] Y. Wang, P. Luo, X. Zheng and B. Zhang, A 0.3V-1.2V ultra-low input voltage, reconfigurable switched-capacitor DC-DC converter for energy harvesting system, *Proc. of the 13th IEEE International Conference on Solid-State and Integrated Circuit Technology*, pp.1333-1335, 2016.
[23] A. Mahmoud, M. Alhawari, B. Mohammad, H. Saleh and M. Ismail, A charge pump based power management unit with 66%-efficiency in 65 nm CMOS, *Proc. of IEEE International Symposium on Circuits and Systems*, 2018.

[24] Z. Luo, P. Luo, M. D. Ker, W. H. Cheng and T. Y. Yen, Regulated charge pump with new clocking scheme for smoothing the charging current in low voltage CMOS process, *IEEE Trans. Circuits and Systems I: Regular Papers*, vol.64, no.3, pp.528-536, 2017.
[25] X. Jiang, X. Yu, K. Moez, D. G. Elliott and J. Chen, High-efficiency charge pumps for low-power on-chip applications, *IEEE Trans. Circuits and Systems I: Regular Papers*, vol.65, no.3, pp.1143-1153, 2018.
[26] K. Eguchi, H. Fujisaki, S. Padmanaban and I. Oota, Design of a cross-connected charge pump for energy harvesting systems, *Proc. of the 6th International Conference on Power Science and Engineering*, vol.136, 2017.
[27] K. Abe, K. Smerpitak, S. Pongswatd, I. Oota and K. Eguchi, A step-down switched-capacitor AC-DC converter with double conversion topology, *International Journal of Innovative Computing, Information and Control*, vol.13, no.1, pp.319-330, 2017.
[28] K. Abe, W. Do, S. Kittipanyangam, I. Oota and K. Eguchi, A Fibonacci-type DC-AC inverter designed by switched capacitor technique, *International Journal of Innovative Computing, Information and Control*, vol.12, no.4, pp.1197-1207, 2016.
[29] K. Eguchi, A. Wongjan, A. Julsereewong, W. Do and I. Oota, Design of a high-voltage multiplier combined with Cockcroft-Walton voltage multipliers and switched-capacitor AC-AC converters, *International Journal of Innovative Computing, Information and Control*, vol.13, no.3, pp.1007-1019, 2017.
[30] K. Eguchi, P. Julsereewong, A. Julsereewong, K. Fujimoto and H. Sasaki, A Dickson-type adder/subtractor DC-DC converter realizing step-up/step-down conversion, *International Journal of Innovative Computing, Information and Control*, vol.9, no.1, pp.123-138, 2013.

Appendix.

A.1. **Characteristics of Conventional Charge Pump.** In this section of A.1, the conventional charge pumps [15-18] are theoretically analyzed, based on the four-terminal equivalent model in steady state as shown in Figure 3.

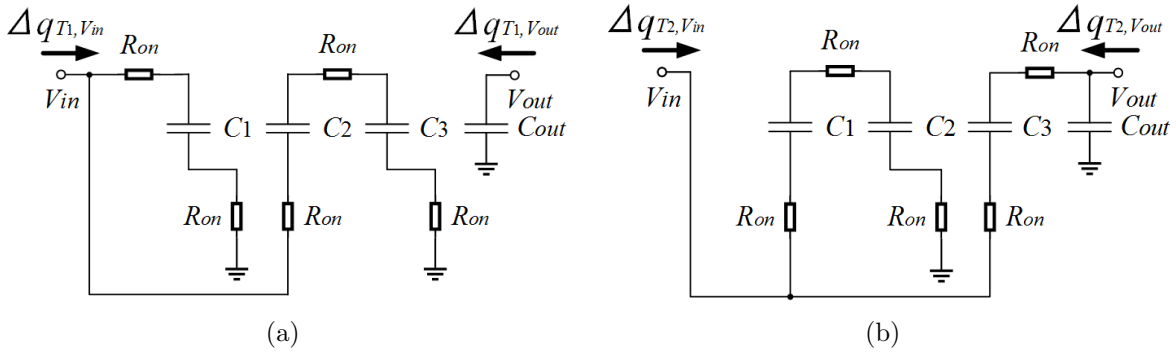

FIGURE 10. Equivalent circuits of the conventional charge pump: (a) state-T_1 and (b) state-T_2

Figure 10 shows equivalent circuits of the conventional charge pump [15-18] in steady state. In Figure 10, the parameter $\Delta q_{T_i,V_{in}\ or\ V_{out}}$ represents the amount of the electric charges of the input or output in state-T_i $(i = 1, 2)$. The parameter R_{on} represents the equivalent resistance of closed switches. By using the ampere-second balance principle and Kirchhoff's current law, we can obtain the following equation in State-T_1.

$$\begin{aligned} \Delta q_{T_1,V_{in}} &= \Delta q^1_{T_1} - \Delta q^2_{T_1}, \\ \Delta q_{T_1,V_{out}} &= \Delta q^{out}_{T_1}, \\ \text{and} \quad \Delta q^2_{T_1} &+ \Delta q^3_{T_1} = 0, \end{aligned} \tag{14}$$

where the parameter $\Delta q^k_{T_i}$ represents the amount of the k-th $(k = 1, 2, 3, out)$ capacitor (C_k)'s electric charges in state-T_i $(i = 1, 2)$.

Likewise, by using the same way in State-T_1, the relationship of electric charges in State-T_2 can be expressed as

$$\begin{aligned} &\Delta q_{T_2,V_{in}} = -\Delta q^1_{T_2} - \Delta q^3_{T_2}, \\ &\Delta q_{T_2,V_{out}} = \Delta q^{out}_{T_2} + \Delta q^3_{T_2}, \\ \text{and} \quad &\Delta q^1_{T_2} + \Delta q^2_{T_2} = 0. \end{aligned} \tag{15}$$

The relationship between the input and output average currents including conversion ratio can be derived as shown in (16) by substituting (14) and (15) into (7) and using the characteristic of the steady state.

$$I_{in} = -4I_{out}. \tag{16}$$

According to (16), the parameter m in Figure 3 is 4.

The next step is to analyze the energy consumption except for the output load in one operation period and to derive the R_{SC}. The energy consumption in State-T_1 is obtained as (17).

$$\begin{aligned} W_{T_1} &= \frac{\left(\Delta q^1_{T_1}\right)^2}{T_1} 2R_{on} + \frac{\left(\Delta q^2_{T_1}\right)^2}{T_1} 3R_{on} \\ \text{and} \quad W_{T_2} &= \frac{\left(\Delta q^1_{T_2}\right)^2}{T_2} 3R_{on} + \frac{\left(\Delta q^3_{T_2}\right)^2}{T_2} 3R_{on}. \end{aligned} \tag{17}$$

From (17), the total energy consumption in one operation period can be derived as (18).

$$W_T = \frac{\left(\Delta q_{V_{out}}\right)^2}{T} 20R_{on}. \tag{18}$$

Therefore, we can confirm by comparing (11) and (18) that the parameter R_{SC} is $20R_{on}$. Through above steps, we can derive the K-matrix of the conventional charge pump as (19), which includes the information of the relation of I/O, the conversion ratio and the internal resistance.

$$\begin{bmatrix} V_{in} \\ I_{in} \end{bmatrix} = \begin{bmatrix} 1/4 & 0 \\ 0 & 4 \end{bmatrix} \begin{bmatrix} 1 & 20R_{on} \\ 0 & 1 \end{bmatrix} \begin{bmatrix} V_{out} \\ -I_{out} \end{bmatrix}. \tag{19}$$

By using (19) and applying the voltage division principle, the maximum power efficiency $\eta_{\max}$ and the maximum output voltage $V_{\max}$ of the conventional charge pump can be derived, which are obtained as Table 1.

A.2. **Characteristics of Series-Parallel Charge Pump.** In this section of A.2, the series-parallel charge pump in Figure 11 [21,22] is theoretically analyzed, based on the four-terminal equivalent model in steady state as shown in Figure 3.

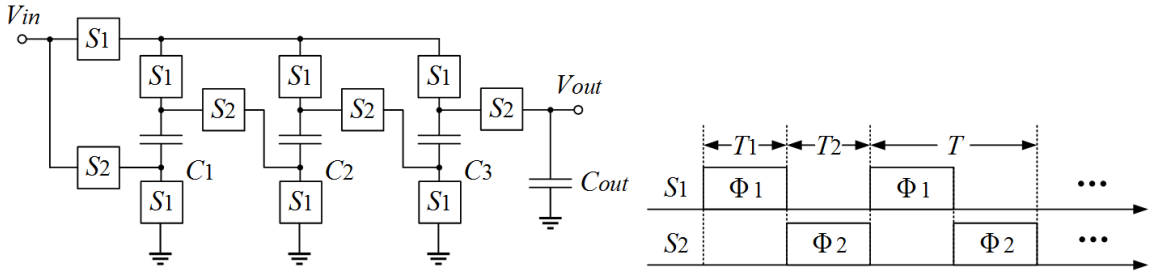

FIGURE 11. Circuit and operation clocks pulses (Φ_1 and Φ_2) of the series-parallel charge pump

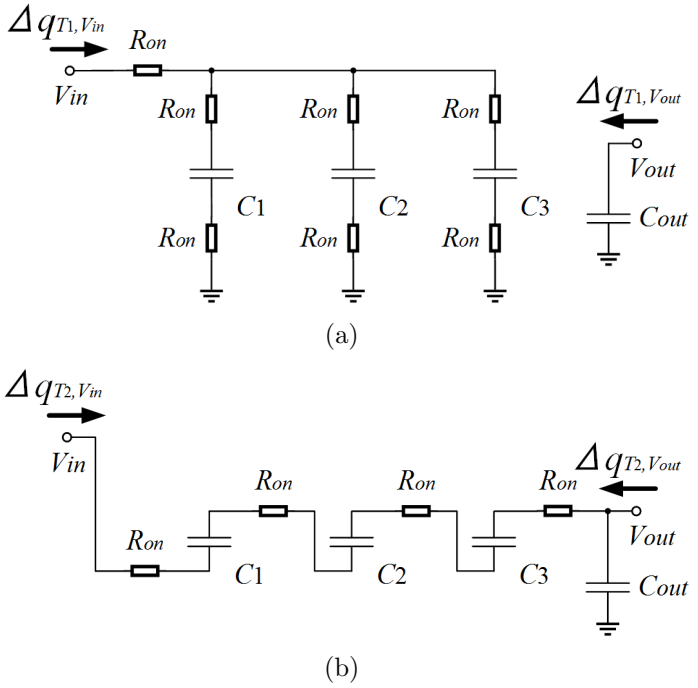

FIGURE 12. Equivalent circuits of the series-parallel charge pump: (a) state-T_1 and (b) state-T_2

Likewise, the theoretical analysis of the series-parallel charge pump satisfies the ampere-second balance principle and Kirchhoff's current law. Therefore, we can derive (20) related to the amount of all components' electric charge in State-T_1 (the capacitors and the input and output in Figure 12).

$$\begin{aligned} & \Delta q_{T_1,V_{in}} = \Delta q^1_{T_1} + \Delta q^2_{T_1} + \Delta q^3_{T_1} \\ \text{and} \quad & \Delta q_{T_1,V_{out}} = \Delta q^{out}_{T_1}, \end{aligned} \tag{20}$$

the parameter $\Delta q^k_{T_i}$ represents the amount of the k-th ($k = 1, 2, 3, out$) capacitor (C_k)'s electric charges in state-T_i ($i = 1, 2$).

By using the same way in State-T_1, the relationship of electric charges in State-T_2 can be expressed as

$$\begin{aligned} & \Delta q_{T_2,V_{in}} = -\Delta q^1_{T_2}, \\ & \Delta q_{T_2,V_{out}} = \Delta q^{out}_{T_2} + \Delta q^1_{T_2}, \\ \text{and} \quad & \Delta q^1_{T_2} = \Delta q^2_{T_2} = \Delta q^3_{T_2}. \end{aligned} \tag{21}$$

The relationship between the input and output average currents including conversion ratio can be derived as shown in (22) by substituting (20) and (21) into (7) and using the characteristic of the steady state.

$$I_{in} = -4I_{out}. \tag{22}$$

According to (22), the parameter m in Figure 3 is 4.

The next step is to analyze the energy consumption except for the output load in one operation period and to derive the R_{SC}. The energy consumption in State-T_1 is obtained as (23).

$$W_{T_1} = \frac{\left(\Delta q^1_{T_1}\right)^2}{T_1} 6R_{on} + \frac{\left(3\Delta q^1_{T_1}\right)^2}{T_1} R_{on}$$
$$\text{and} \quad W_{T_2} = \frac{\left(\Delta q^1_{T_2}\right)^2}{T_2} 4R_{on}. \tag{23}$$

From (23), the total energy consumption in one operation period can be derived as (24).

$$W_T = \frac{\left(\Delta q_{V_{out}}\right)^2}{T} 38R_{on}. \tag{24}$$

Therefore, we can confirm by comparing (11) and (24) that the parameter R_{SC} is $38R_{on}$. Through above steps, we can derive the K-matrix of the conventional charge pump as (25), which includes the information of the relation of I/O, the conversion ratio and the internal resistance.

$$\begin{bmatrix} V_{in} \\ I_{in} \end{bmatrix} = \begin{bmatrix} 1/4 & 0 \\ 0 & 4 \end{bmatrix} \begin{bmatrix} 1 & 38R_{on} \\ 0 & 1 \end{bmatrix} \begin{bmatrix} V_{out} \\ -I_{out} \end{bmatrix}. \tag{25}$$

By using (25) and applying the voltage division principle, the maximum power efficiency $\eta_{\max}$ and the maximum output voltage $V_{\max}$ of the series-parallel charge pump can be derived, which are obtained as Table 1.